# Accurate Determination of the Ionization Energy in Pixelated TlBr Correcting for Charge Collection Efficiency

Sean O'Neal, Zhong He, *Senior Member*, Charles Leak, Hadong Kim, Leonard Cirignano, and Kanai Shah

***Abstract*—Thallium-bromide (TlBr) is currently under investigation for use as an alternative room-temperature semiconductor gamma-ray spectrometer. Performance of better than 1% FWHM at 662 keV can be achieved when TlBr detectors are cooled to $-20^{\circ}C$. The theoretical limit of energy resolution is determined by the ionization energy in semiconductor detectors, and accurately measuring it is important for determining the best possible performance. One method to determine the ionization energy of semiconductor detectors compares pulse heights obtained from the semiconductor to pulse heights from a silicon detector. Due to their higher trapping, the charge collection efficiency (CCE) of TlBr is significantly lower than it is in silicon, therefore a correction to the ionization energy must be made. In this work, we present the theory and measurement for accurately determining the CCE using the Shockley-Ramo theorem and apply it to measurement of ionization energy in pixelated TlBr detectors. The ionization energy of two TlBr detectors is measured and found to be 4.83(8) eV and 5.49(10) eV for the two samples at room temperature and $-20^{\circ}C$ respectively.**

***Index Terms*—TlBr, room-temperature semiconductors, pixelated detectors, ionization energy.**

## I. Introduction

THALLIUM-BROMIDE (TlBr) is currently under investigation for use as a room-temperature semi-conductor gamma-ray spectrometer due to its wide band gap and high stopping power. Additionally, due to its low melting point and simple cubic structure, simple melt-based techniques such as the traveling molten zone (TMZ) method can be used for growth and purification [1]. Many researchers have grown large boules with high resitivity ($\rho > 10^{10}\Omega cm$) and demonstrated good electron mobility-lifetime products ($\mu\tau_e > 10^{-3}cm^2/V$) in up to 5 mm thick detectors [1]-[3]. With these samples, good performance has been demonstrated in both room-temperature and near room temperature operation [4]-[6].

Single-pixel performance better than 1% FWHM at 662 keV has been achieved in TlBr devices, but these results have been limited to cooled operation at $-20^{\circ}C$ [4],[7]. At room-temperature, the device degrades as a results of ionic conduction [8]. Recent developments in surface preparation techniques have extended the room-temperature lifetime of TlBr detectors from a few days to greater than 100 days [5],[9].

S. O'Neal, Z. He, and C. Leak are with the Department of Nuclear Engineering and Radiological Sciences, University of Michigan, Ann Arbor, MI, 48109 USA email:onealsp@umich.edu

H. Kim, L. Cirignano, and K. Shah are with Radiation Monitoring Devices Inc., Watertown, MA 02472 USA.

Manuscript Submitted 15 September 2017, revised 14 December 2017

To determine the best possible energy resolution in semiconductor detectors, the ionization energy of the material must be measured. The ionization energy of TlBr has been reported by multiple researchers. Shah, et al., determined a value of 6.5 eV in 1989 [10] and Hitomi, et al., determined a value of 5.5 eV in 2015 [11]. Both of these results were measured by comparing the signal amplitude in TlBr to the signal amplitude in another material at room temperature.

A reduction in the measured ionization energy as material purity increases is not uncommon [11], but this is because the trapping in the material is not properly accounted for when determining the ionization energy. Hitomi, et al., proposed correcting the observed signal by the measured charge collection efficiency (CCE) to determine the intrinsic material parameter of the ionization energy, which determines the true limiting performance of the detector [11].

In their work, Hitomi, et. al, applied the traditional Hecht relation to a pixelated detector, which does not properly model the trapping, resulting in an under estimation of the $\mu_e\tau_e$ product [11]. Fortunately, due to the low trapping, the estimation of the CCE is still very accurate and the results from Hitomi, et al. are still reliable.

In this work, we experimentally determine the ionization energy in TlBr at both room-temperature and at $-20^{\circ}C$. In both measurements, we determined the CCE by a modified Hecht relation for pixelated detectors and the two-bias method using the updated correction for non-ideal weighting potentials as reported in Ref [12] and corrected the measured ionization energy.

## II. Methods

### A. Experimental Setup

The TlBr detectors reported in this work were grown by Radiation Monitoring Devices (RMD). The material was purified and grown using the TMZ method and an approximately 5 mm x 5 mm x 5 mm cube was cut from the resulting boule. Detector 1 was then etched with HCl and platinum electrodes were deposited by electron-beam at Lawrence Livermore National Lab. More information about the detector fabrication and performance can be found in Ref [5]. Detector 2 was etched with Br-Methanol and Cr/Au electrodes were deposited by vapor deposition at RMD, Inc.

Each detector has a three-by-three pixelated anode with a 0.9 x 0.9 $mm^2$ pixel pad with 1 mm pitch and a planar cathode. A 0.5 mm thick guard ring surrounds all the anode

This article has been accepted for publication in a future issue of this journal, but has not been fully edited. Content may change prior to final publication. Citation information: DOI 10.1109/TNS.2018.2804038, IEEE Transactions on Nuclear Science



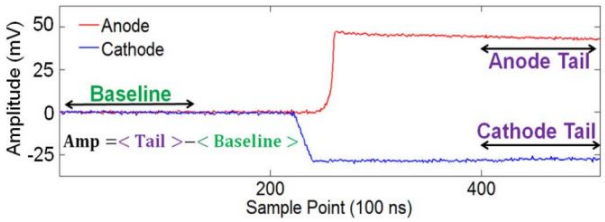


Fig. 1. Example of 100 point simple subtraction

pixels. The signal from each electrode was read out using eV-Products 509 charge-sensitive preamplifiers whose outputs were digitized by 14-bit GaGe Octopus CompuScope PCIe digitizers. For each waveform, 512 samples were recorded at a sampling frequency of 10 MHz. The detector was cathode-biased to -1000V (unless otherwise noted) and irradiated from the cathode side with $^{241}Am$ gamma rays. For the cooled work, the detector testing was done in a Thermotron S-1.2-3200 environmental chamber.

The silicon detector in this work was a Hamamatsu PIN diode (S1223). The diode bias was set so full charge collection was achieved within 10 $\mu s$ ($\sim$30 V) and was irradiated with $^{241}Am$ gamma rays. The signal was read out using the same preamplifiers and digitizer settings as the TlBr detectors.

### B. Digital Pulse Processing

The amplitude of each measured waveform was determined by simple subtraction (see Fig. 1). 100 data points were used for both the baseline and tail regions of the waveforms. The same processing method was used for both TlBr and Si waveforms.

The example waveform in Fig. 1 shows a small amount of preamplifier decay over the sampling time (51.2 $\mu s$). Since the same sampling time was used for both TlBr and Si, and the rise time of the pulses were similar, it was assumed that the amount of preamplifier decay for both materials was the same.

### C. Determination of the Ionization Energy

The ionization energy of TlBr was determined by comparing the pulse height from $^{241}Am$ in TlBr to that in Si and correcting for charge collection efficiency (CCE). Due to the very high $\mu\tau$ product in Si, the CCE was assumed to be unity for Si. The ionization energy of TlBr, $w_{TlBr}$ can then be determined by Eq. 1.

$$w_{TlBr} = CCE_{TlBr}\frac{A_{Si}}{A_{TlBr}}w_{Si} \tag{1}$$

Where $A_{Si}$ and $A_{TlBr}$ are the $^{241}Am$ signal amplitudes in Si and TlBr respectively and $w_{Si}$ is the ionization energy of silicon, taken to be 3.67(2) eV from Ref [13]. For an ideal pixelated weighting potential, the CCE can be calculated if the $\mu\tau$-product is known.

$$CCE = \frac{N}{N_0} = e^{-t/\mu\tau E} \tag{2}$$

Where t is the thickness, E is the electric field, $N_0$ is the initial number of charges and N is the number of charges which reach the anode. The $\mu\tau$-product can be calculated in multiple ways including a fit to a modified Hecht relation or the two bias method.

*1) Two-bias Method:* Using the two-bias method, the $\mu\tau$-product can be calculated by

$$\mu_e\tau_e = k\frac{t^2}{ln(\frac{N_1}{N_2})}\Big(\frac{1}{V_2} - \frac{1}{V_1}\Big). \tag{3}$$

Where $N_1$ and $N_2$ are the signal amplitudes at two different biases $V_1$ and $V_2$ and k is a correction factor which accounts for the non-ideal weighting potential in pixelated detectors as discussed by Koehler, et. al [12].

*2) Modified Hecht Relation:* In general, the induced charge, Q, from a drifting charge, q, is given by the Shockley-Ramo theorem, as

$$Q = \int_{x_0}^{x_f} -q(x)\frac{\partial\psi_0(x)}{\partial x}dx \tag{4}$$

where $\psi_0$ is the weighting potential and $x_0$ and $x_f$ are the initial and final positions respectively. The drifting charge varies along its path due to trapping given by

$$q(x) = Q_0 e^{(x_0-x)/\mu_e\tau_e E} = Q_0 e^{(x_0-x)t/\mu_e\tau_e V} \tag{5}$$

where $Q_0$ is the initial number of charges created by the incident gamma-ray. Combining Eqs. 4 and 5 and assuming the interaction occurs on the cathode side ($x_0$ = 0), the CCE can be expressed as

$$CCE = \frac{Q}{Q_0} = \int_t^0 -e^{(x_0-x)t/\mu_e\tau_e V}\frac{\partial\psi_0(x)}{\partial x}dx. \tag{6}$$

In the case of a linear weighting potential, this reduces to the traditional Hecht relation as applied by Hitomi, et. al [11].

$$CCE_{planar} = \int_t^0 -e^{(x_0-x)t/\mu_e\tau_e V}\frac{1}{t}dx = \frac{\mu_e\tau_e V}{t^2}(1-e^{-t^2/\mu_e\tau_e V}) \tag{7}$$

For ideal pixelated detectors, the weighting potential is zero throughout the bulk and sharply increases to unity at the anode surface, so the CCE is instead given by

$$CCE_{ideal} = \int_t^0 -e^{(x_0-x)t/\mu_e\tau_e V}\delta(x)dx = e^{-t^2/\mu_e\tau_e V}. \tag{8}$$

Eq. 8 represents the modified Hecht relation for pixelated detectors. A more accurate determination of the $\mu\tau$-product can be made by accounting for the non-ideal part of the weighting potential by solving Eq. 6 using a numeric solution for the weighting potential in the detector determined using the exact detector geometry.

This article has been accepted for publication in a future issue of this journal, but has not been fully edited. Content may change prior to final publication. Citation information: DOI 10.1109/TNS.2018.2804038, IEEE Transactions on Nuclear Science



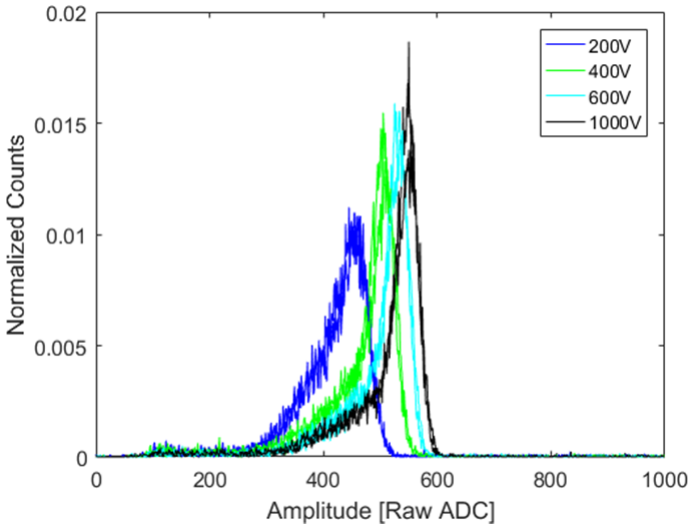


Fig. 2. $^{241}Am$ spectrum in TlBr detector 1 (pixel 3) for multiple detector biases.

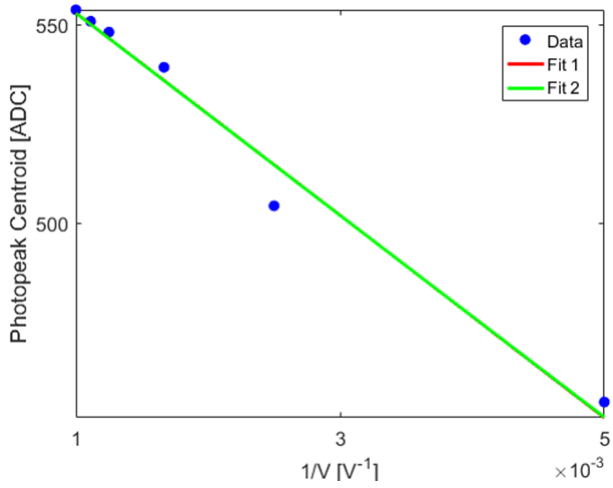


Fig. 3. Photopeak centroid versus inverse bias for TlBr detector 1 showing fits for both the classic Hecht relation (Eq. 7) and the modified Hecht relation (Eq. 8). (Note: these fits are very similar and overlap in the figure).

## III. Results

### A. Room Temperature - Detector 1

Fig. 2 shows the $^{241}Am$ spectrum from an example pixel of TlBr detector 1 at multiple different biases with Fig. 3 showing the centroid versus bias fit by both the classic Hecht relation (Fit 1, Eq. 7) and the modified Hecht relation for pixelated detectors (Fit 2, Eq. 8). (Note: these fits are very similar and overlap in Fig. 3).

Table I shows the fit parameters for three different fits to the centroid versus bias for the detector. These are the two fits shown in Fig. 3 and a third one using the exact weighting potential of the pixelated detector. These fits show very close values for the CCE, though they vary greatly in their calculated $\mu_e\tau_e$-product. This shows that the results from Hitomi et al. [11] for the ionization energy are reliable even though the wrong model for trapping was used.

TABLE I
Fit Parameters

| Fit Type | $\mu_e\tau_e$ [$10^{-3}$ cm$^2$/Vs] | CCE at 1000 V |
|---|---|---|
| Ideal WP | 4.0 | 0.954 |
| Exact (Numerical) WP | 3.6 | 0.954 |
| Classic Hecht (Linear WP) | 1.9 | 0.952 |

Table II shows the calculation of the ionization energy from 4 pixels of detector 1 at room-temperature, where $w_{eff}$ is the uncorrected ionization energy, and w is the true ionization energy as calculated using Eq. 1 corrected with the CCE determined using the true weighting potential. Results are only available for these four pixels due to high electronic noise in some pixels and some attenuation from the detector substrate board preventing good TlBr spectra on other pixels.

The ionization energy in detector 1 was determined to be 4.83(8) eV at room temperature.

### B. Cooled ($-20°C$) - Detector 2

Detector 2 operated at $-20°C$ and the CCE was calculated from the $\mu_e\tau_e$-product determined by the two-bias method (see Eq. 3 using the proper correction factor for the exact detector geometry as reported in Ref [12]). The silicon signal amplitude was also recorded at $-20°C$ to account for any drift in the preamplifiers with temperature. Table III shows the results from detector 2.

The ionization energy in detector 2 was determined to be 5.49(10) eV at $-20°C$.

### C. Comparison of Results

The two measurements of the ionization energy do not agree within error, though each detector showed stable signal amplitudes and reproducible results. It is possible that the ionization energy of TlBr can change with temperature. Detector 1 represents new TlBr material which has been optimized for room-temperature operation in both its growth and fabrication. These type of detectors are not stable when cooled, so cooled operation would not yield reproducible results. Consequently, a direct comparison of the ionization energy in this detector with temperature is not possible. Detector 2 represents older TlBr material which polarizes very quickly (a few hours to a few days) at room temperature, so any measurement at room temperature with it will not be repeatable, and again a direct comparison cannot be made.

In the determination of the cooled ionization energy, the ionization energy of Si was assumed to be constant with temperature. The ionization energy does increase very slightly as the temperature decreases, increasing by 4% between room temperature and 77 K [14]. This would indicate that the cooled ionization energy could be slightly higher than reported here, but this does not account for the large difference observed between the two temperatures.

### D. Prediction of Limiting Energy Resolution

Using the ionization energy the theoretical limiting energy resolution can be estimated.

$$R_{limit} = 2.35\sqrt{\frac{Fw}{E}} \quad (9)$$

TABLE II
IONIZATION ENERGY IN DETECTOR 1

| Pixel | $A_{Si}$ [ADC] | $A_{TlBr}$ [ADC] | CCE at 1000V | $w_{eff}$ [eV] | w [eV] |
|---|---|---|---|---|---|
| 1 | 767.06 | 541.1 | 0.948 | 5.20 | 4.93 |
| 3 | 768.03 | 553.94 | 0.954 | 5.09 | 4.85 |
| 4 | 754.99 | 556.84 | 0.960 | 4.98 | 4.78 |
| 6 | 752.02 | 549.95 | 0.948 | 5.02 | 4.76 |
| | | | Average: | 5.07(10) | 4.83(8) |

TABLE III
IONIZATION ENERGY IN DETECTOR 2

| Pixel | $A_{Si}$ [ADC] | $A_{TlBr}$ [ADC] | $\mu_e\tau_e$ $[10^{-3}\ cm^2/Vs]$ | CCE at 1000 V | $w_{eff}$ [eV] | w [eV] |
|---|---|---|---|---|---|---|
| 1 | 256.7 | 161.0 | 4.2 | 0.94 | 5.85 | 5.51 |
| 3 | 254.1 | 165.9 | 10 | 0.97 | 5.62 | 5.49 |
| 4 | 248.9 | 165.0 | 6.4 | 0.96 | 5.53 | 5.32 |
| 6 | 256.0 | 170.9 | 12 | 0.98 | 5.58 | 5.47 |
| 8 | 259.8 | 169.0 | 12 | 0.98 | 5.64 | 5.53 |
| 9 | 250.2 | 158.9 | 11 | 0.98 | 5.78 | 5.64 |
| | | | | Average: | 5.67(12) | 5.49(10) |

Where F is the Fano factor and E is the energy of the gamma-ray. The Fano factor depends on the exact phonon energy levels in the material and thus can vary between different detector materials [15]. Without measuring phonon levels, a simplified model for the Fano factor can be used resulting in Eq. 10 [16].

$$F \approx \frac{1}{6}\Big(\frac{w - E_{gap}}{w}\Big)^2 \tag{10}$$

Using Eq. 10, the Fano factor of Si is estimated to be 0.07. This result is much lower than many reported values [17], but the Fano factor in Si is known to vary with X-ray energy which is an effect not included in the model used to generate Eq. 10 [16], [17]. However, Eq. 10 predicts a value of 0.09 for Ge, which is close to some reported values [18].

Consequently, Eq. 10 may not accurately predict the actual Fano factor in each material, but it and the theory behind it does indicate that a lower Fano factor in TlBr can be expected because the lower ratio between the band gap and ionization energy.

Table IV shows a comparison of the theoretical limiting energy resolution of TlBr to CZT at 662 keV using the CZT ionization energy reported in Ref [14] and the cooled ionization energy from this work. Because the ratio of the ionization energy to band gap in TlBr is much lower, the limiting energy resolution is better in TlBr than in CZT even due to its wider band gap.

Though both materials are currently limited by material non-uniformity and electronic noise, and detailed study of the phonon modes in TlBr is needed to more accurately estimate the Fano Factor in TlBr, this demonstrates that TlBr could be capable of comparable energy resolution to that of CZT as the material continues to improve.

## IV. CONCLUSION

The ionization energy of two TlBr detectors was measured and found to be 4.83(8) eV at room temperature and 5.49(10) eV at $-20°C$ when corrected for charge collection efficiency. The higher value agrees with the previously reported value by Hitomi et. al. [11], and the variation between the two measurements may be due to both material differences and the temperature.

TABLE IV
COMPARISON OF THEORETICAL LIMIT OF RESOLUTION IN TLBR AND CZT AT 662 KEV

| Material | CZT | TlBr |
|---|---|---|
| Band Gap [eV] | 1.64 | 2.68 |
| W [eV] | 4.6 | 5.49 |
| $F_{theory}$ | 0.069 | 0.044 |
| $R_{limit}$ at 662 keV | 0.16% | 0.14% |

The charge collection efficiency was determined both by Hecht fitting and the two-bias method with the correction factor for non-ideal weighting potentials. Due to the low trapping in these detectors, the charge collection efficiency was demonstrated to not be a strong function of the trapping model, though using the proper trapping model is important for precise determination of the $\mu_e\tau_e$-product.

The ratio of the ionization energy to the band gap in TlBr is much lower than in many other semiconductor materials (at $\sim$2 to 1, instead of $\sim$3 to 1), and this causes the theoretical limiting energy resolution of TlBr to be similar to that of CZT even though it has a much wider band gap.

## ACKNOWLEDGMENT

The authors would like to thank Adam Conway at LLNL for fabricating TlBr detector 1. This work was funded by DNDO of DHS under a subcontract through Radiation Monitoring Devices, Inc. (Contract #HSHQDN-16-C-00024).

## REFERENCES

[1] A. V. Churilov, W. M. Higgins, G. Ciampi, H. Kim, L. J. Cirignano, F. Olschner, and K. S. Shah, "Purification, crystal growth and detector performance of TlBr," *Proc. SPIE*, vol. 7079, p. K1-K8, 2008.

[2] H. Kim, L. Cirignano, A. Churilov, G. Ciampi, W. Higgins, F. Olschner, and K. Shah, "Developing larger TlBr detectors: Detector performance," *IEEE Trans. Nucl. Sci.*, vol 56, no.3, 2009.

[3] K. Hitomi, T. Onodera, T. Shoji, and Z. He, "Pixellated TlBr detectors with the depth sensing technique," $Nucl.\ Instr.\ Meth.\ A$, vol. 578, pp. 235-238, Jul. 2007.

[4] C. Thrall, W. Kaye, Z. He, H. Kim, L. Cirignano, and K. Shah "Transient behavior in TlBr gamma-ray detectors and its analysis using 3-d position sensing" $IEEE\ Trans.\ Nucl.\ Sci.$, vol 60, no. 2, 2013.

[5] S. O'Neal, W. Koehler, Z. He, H. Kim, L. Cirignano, K. Shah, A. Conway, E. Swanberg, L. Voss, R. Graff, A. Nelson, and S. Payne, "Improvements in room temperature lifetime of pixelated TlBr detectors from surface etching," 2015 $IEEE\ NSS/MIC$, San Diego, CA, 2015.

[6] K. Hitomi, T. Onodera, S. Kim, T. Shoki, and K. Ishii, "Characterization of pixelated TlBr detectors with Tl electrodes," $Nucl.\ Instr.\ Meth.\ A$, vol. 747, pp. 7-12, Feb. 2014.

[7] W. Koehler "Thallium Bromide as an Alternative Material for Room-Temperature Gamma-Ray Spectroscopy and Imaging " Ph. D. Thesis, University of Michigan, 2014.

[8] W. Koehler, Z. He, C. Thrall, S. O'Neal, H. Kim, L. Cirignano, and K. Shah "Quantitative investigation of room-temperature breakdown effects in pixelated TlBr detectors" $IEEE\ Trans.\ Nucl.\ Sci.$, vol 60, no. 2, 2013.

[9] A. Conway, L. Voss, A. Nelson, P. Beck, T. Laurence, R. Graff, R. Nikolic, S. Payne, H. Kim, L. Cirignano, and K. Shah, "Fabrication methodology of enhanced stability room temperature TlBr gamma detectors" $IEEE\ Trans.\ Nucl.\ Sci.$, vol 60, no. 2, 2013.

[10] K. S. Shah, J. C. Lund, F. Olschner, L. Moy, and M. R. Squillante, "Thallium bromide radiation detectors," $IEEE\ Trans.\ Nucl.\ Sci.$, vol. 36, no. 1, Feb. 1989.

[11] K. Hitomi, T. Onodera, S. Kim, T. Shoji, and K. Ishii, "Experimental determination of the ionization energy in TlBr," $IEEE\ Trans.\ Nucl.\ Sci.$, vol. 62, no. 3, June 2015.

[12] W. Koehler, M. Streicher, S. O'Neal, and Z. He, "A correction factor to the two-bias method for determining the mobility-lifetime product in pixelated detectors," $IEEE\ Trans.\ Nucl.\ Sci.$, vol. 63, no. 3, June 2016.

[13] R. H. Pehl, F. S. Goulding, D. A. Landis, and M. Lenzlinger, "Accurate determination of the ionization energy in semiconductor detectors," $Nucl.\ Instrum.\ Methods$, vol. 59, no. 1, pp. 4555, Feb. 1968.

[14] G. F. Knoll, $Radiation\ Detection\ and\ Measurement$, 4th ed. New York: Wiley, 2011.

[15] C. A. Klein, "Bandgap dependence and related features of radiation ionization energies in semiconductors," $J.\ of\ App.\ Physics$, vol. 39, no. 4, pp. 2029-2038, March 1968.

[16] G. D. Alkhazov, A. P. Komar, and A. A. Vorob'ev, "Ionization fluctuations and resolution of ionization chambers and semiconductor detectors," $Nucl.\ Instr.\ Meth.\ A$, vol. 48, pp. 1-12, Feb. 1967.

[17] F. Perotti, and C. Fiorini, "Observed energy dependence of Fano factor in silicon at hard X-ray energies," $Nucl.\ Instr.\ Meth.\ A$, vol. 423, pp. 356-363, 1999.

[18] R.H. Pehl, and F.S. Goulding, "Recent observations on the Fano factor in germanium," $Nucl.\ Instr.\ Meth.$, vol. 81, pp. 329-330, 1970.

[19] Z. He, "Review of the Shockley-Ramo theorem and its application in semiconductor gamma-ray detectors," $Nucl.\ Instr.\ Meth.\ A$, vol. 463, pp. 250-267, Nov. 2000.